



SCICON 2016

## Surface protection of copper in 3% NaCl solution by using 1-(n-butyl)imidazole self-assembled monolayer

P. Durainatarajan<sup>a</sup>, M. Prabakaran<sup>b</sup>, S. Ramesh<sup>a,\*</sup>, V. Periasamy<sup>a</sup>

<sup>a</sup>Department of Chemistry, The Gandhigram Rural Institute-Deemed University, Gandhigram, Tamil Nadu, India-624 302

<sup>b</sup>Department of Chemistry, Gnanamani College of Technology, Tamil Nadu, India-637 018

---

### Abstract

This paper describes the formation of self-assembled monolayer of 1-(n-butyl)imidazole (BI) on electrode surface by self-assembly technique. Electrochemical impedance spectroscopy was conducted to establish the optimum concentration and assembling time of the BI SAM for the SAM formation. It was found that the BI monolayer was formed with the concentration of 1.0 mM of BI at 24 h assembling time and the maximum inhibition efficiency that could be attained is 93.2%. The resulting monolayer was characterized by Fourier transform infrared spectroscopy (FT-IR) and energy dispersive X-ray (EDX) analysis. The surface analysis confirmed that the BI molecule was self-assembled on the copper surface. The corrosion resistance ability of the SAM coated copper in 3% NaCl solution was investigated by potentiodynamic polarization studies, cyclic voltammetry, scanning electron microscopy. The result showed that the presence of BI monolayer on copper electrode resulted in better corrosion resistance against copper corrosion in NaCl medium.

© 2017 Elsevier Ltd. All rights reserved.

Selection and/or Peer-review under responsibility of International Conference on Advanced Materials(SCICON '16).

*Keywords:* Copper; Self-assembled monolayer; 1-(n-butyl)imidazole; Corrosion

---

\* Corresponding author. Tel.: +91 0451 2452371; fax: +91 0451 2454466.

E-mail address: [drsramesh\\_56@yahoo.com](mailto:drsramesh_56@yahoo.com)

## 1. Introduction

Self-assembled monolayers (SAMs) are dense and ordered organic films formed by chemisorption of reactive surfactant on the surface which offers flexible method for the control of structure and interfacial properties [1]. Self-assembly technique is a convenient method for the surface modification against metal corrosion, because of the densely packed and uniform films formed on the metal surface. The ultrathin layer provided by the SAM could act as an effective barrier to block the penetration of corrosive active species like water, oxygen and aggressive ions to the metal surface [2-4]. Copper is a prime metal widely used in various range of applications due to its anomalous properties such as high electrical as well as thermal conductivity and excellent mechanical workability. However, Copper is very liable to corrosion when exposed to aqueous chloride environment and leads to huge economic losses and various potential safety issues [5-6]. Therefore, protection of copper surface against corrosion has become a major problem in a corrosive environment. Prevention of copper corrosion against aggressive environment using several types of organic compounds have been reported based on the SAM on copper surface such as alkanethiols, alkyl thiosulfate, aromatic thiol, schiff bases, amino acids, organo silane and phytic acid [7–15]. Organic heterocyclic molecules possessing N, S, and O atoms, polar head groups and pi-electron in the heterocyclic ring that bind with surface of metal, can effectively inhibit the metal corrosion as a result of insulating film on the surface, which prevent the communication between metal and corrosive medium [16]. Therefore, heterocyclic compounds such as azoles and its derivatives can provide a possibility to develop a protective layer on surface to prohibit copper corrosion. For instance, Wang et al. compared the inhibition efficiencies of two kinds of self-assembled films viz., carbazole and N-vinyl carbazole on copper surface. Their inhibition efficiencies were reported as 91.1% and 93.4%, respectively [2]. Chen et al. studied the protection of copper from corrosion in 0.5 M sodium chloride solution using 5-mercapto-3-phenyl-1,3,4-thiadiazole-2-thione potassium self-assembled monolayer [3]. Appa Rao et al. studied the self-assembled monolayer of 5-methoxy-2-(octadecylthio) benzimidazole and 1-octadecyl-1H-imidazole on copper surface for corrosion protection [17,18].

Nowadays, the increasing strict regulations and concerns for environmental safety as well as potential health hazard associated with a number of corrosion inhibitors, their use is being limited. Therefore, finding the new kind of less or non-toxic inhibitor molecules for surface modification for the protection of copper from corrosion is a significant task for the researchers. Imidazole derivatives have been studied for their excellent inhibitor properties against the corrosion of copper in neutral media and is also a non-toxic inhibitor [19,20].

Even though, few literatures were reported for the copper protection against corrosion using non-toxic compound as self-assembled monolayer on copper surface, to the best of our knowledge, there is no report in the literature using 1-(3-aminopropyl) imidazole (BI) as a monolayer for the protection of copper corrosion. Hence, we made an attempt to form BI SAM on copper surface by self-assembly technique. In the current study, one of the imidazole derivatives of BI was self-assembled on copper surface to inhibit corrosion of copper in 3% NaCl solution. The formation of the BI SAM on substrate surface was characterized by Fourier transform infrared spectroscopy and energy dispersive X-ray analysis while corrosion resistance performance of the BI SAM was assessed by potentiodynamic polarization, cyclic voltammetry, scanning electron microscopy in 3% NaCl solution.

## 2. Experimental section

### 2.1. Materials

1-(3-aminopropyl)-2-methyl-1H-imidazole (Sigma–Aldrich, 97%), sodium chloride (Merck, 99%), and absolute ethyl alcohol (Merck, 99.9%) were used as received without further purification. The testing solution of 3% NaCl was prepared by dissolving an analytical reagent of sodium chloride in double distilled water. Concentration range of the BI solutions used for the experiments was 0.1 to 1.0 mM.

### 2.2. Preparation of electrodes

The working electrode was prepared from copper sheet with 99.9% purity. The electrode was insulated with Teflon sheath and working area of surface exposed to the solution was 1 cm<sup>2</sup> for the electrochemical experiments.

Before all the experiments, the exposed surface of the electrode was mechanically abraded with various grades of emery paper (up to 4/0), followed by fine polishing with alumina slurries (down to 0.3  $\mu\text{m}$ ) on a felt cloth until smooth, shiny surface was obtained. Then, it was rinsed with distilled water, degreased with absolute ethyl alcohol in an ultrasonic bath for 5 min to remove any possible residue during the pre-treatment process, and dried in the  $\text{N}_2$  atmosphere.

### 2.3. Formation of BI SAM on copper

The freshly prepared electrodes were rapidly immersed in the BI ethanol solution at different concentrations (0.1 to 1.0 mM) and different self-assembly periods (1 to 30 h) for forming self-assembled monolayer at room temperature. Afterward formation of the film, the modified electrodes were removed from the BI solution and rinsed adequately with ethanol followed by double distilled water to remove the physically detached molecules on the electrode surface and dried by flowing  $\text{N}_2$  gas and then used for further investigation.

### 2.4. Electrochemical techniques

The electrochemical corrosion tests were conducted with a CHI760D electrochemical analyzer in a standard three electrode electrochemical cell configurations, wherein a saturated calomel electrode (SCE) and platinum electrode (Pt) were employed as the reference electrode and auxiliary electrode, respectively. The bare copper electrode or SAM coated copper electrode was served as the working electrode (WE). All reported potential values in this work with reference to SCE. Before each experiment, the copper electrode was immersed in a test solution for 60 min to establish steady state open circuit potential (OCP). The impedance measurements were carried out at the open circuit potential with the AC amplitude of 5mV in the frequency range from 100 kHz to 0.1 Hz. Then the EIS data were collected and analysis were performed using ZSimpWin 3.21 software and fitted to the compatible electrical equivalent circuits. The fitting results gave the values of the elements in the electrical equivalent circuits. Tafel polarization curves were obtained from  $\pm 250$  mV vs. OCP with a scan rate of 2 mV  $\text{s}^{-1}$ . Cyclic voltammogram curves were recorded in the scan range of -0.6 V (SCE) to +0.6 V (SCE) with a scan rate of 20 mV  $\text{s}^{-1}$  in test solution. All electrochemical experiments were conducted at room temperature and performed at least thrice for reproducibility.

### 2.5. Sample characterization

Fourier transform infrared (FT-IR) spectra were recorded on a FTIR spectrometer (JASCO 460+ Spectrophotometer) in the wave number range of 4000–400  $\text{cm}^{-1}$ . The surface morphologies characterizing changes of the copper surface were observed by scanning electron microscopy (VEGA3 TESCAN), SEM equipped with an energy dispersive X-ray spectroscopy (Bruker Nano, Germany) (EDS) was used for elemental analysis on the copper substrate surface.

## 3. Results and discussion

### 3.1. Characterization of BI monolayer

It is seen from the Fig. 1, the morphology of newly polished copper surface (Fig. 1a) looks to be a smooth surface with some polishing scratches and nicks while SAM coated surface (see Fig. 1b) showed protective layer cover of copper surface which indicate the successful surface modification on the copper surface. Fig. 2a and b shows the EDX spectra of newly polished and BI SAM modified copper surfaces, respectively. Fig. 2a displays the two peaks corresponding to oxygen (10.52 at.%) at 0.53 keV, and Cu (89.48 at.%) at 0.93 and 8.05 keV, respectively. The modified surface (Fig. 2b) shows peaks due to C (35.91 at.%) at 0.28 keV, N (11.56 at.%) at 0.39 keV, O (22.87 at.%) at 0.53 keV and Cu (29.66 at.%) at 0.93 and 8.05 keV. The existence of C, N and O elements peaks on the surfaces reveals that the BI molecule had been assembled on the copper surface.

Fourier transform infrared spectroscopy (FT-IR) is a powerful technique to confirm the formation of film on the substrate surface. FT-IR spectra of pure BI and copper assembled in 1.0 mM BI solution for 24 h are displayed in Fig.3. The FT-IR spectrum of the pure BI (Fig. 3a) shows two adsorption bands at 2871 and 2935  $\text{cm}^{-1}$  that correspond to  $\text{CH}_2$  symmetric stretching and asymmetric stretching, the band at 2959  $\text{cm}^{-1}$  corresponds to  $\text{CH}_3$  stretching, the bands at 1542 and 1392  $\text{cm}^{-1}$  correspond to  $\nu(\text{C}=\text{N})$  and  $\nu(\text{C}-\text{N})$  of imidazole ring, respectively. On the other hand, BI modified copper (Fig 3b) shows an appreciable shifting of characteristic  $\text{C}=\text{N}$  stretching band from 1542 to 1509  $\text{cm}^{-1}$  and  $\text{C}-\text{N}$  stretching band shifting from 1375 to 1360  $\text{cm}^{-1}$ , revealing that the BI molecule were chemisorbed on copper surface by the nitrogen atom in imidazole. The band at 2855 and 2924  $\text{cm}^{-1}$  correspond to  $\text{CH}_2$  symmetric stretching and asymmetric stretching mode and the band at 2961  $\text{cm}^{-1}$  corresponds to  $\text{CH}_3$  stretching. These peaks are clear evidence for the hydrocarbon chain present on the copper surface.

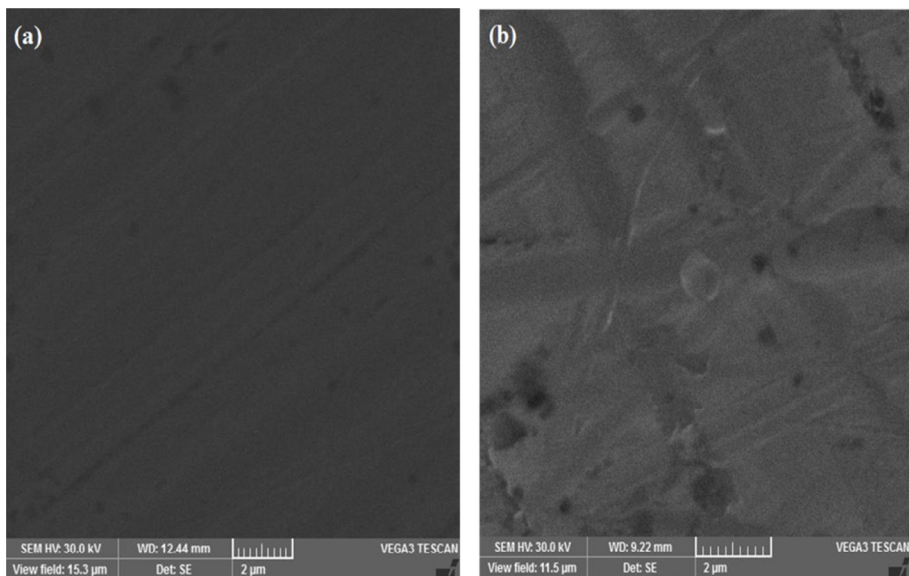


Fig. 1. SEM images of (a) polished and (b) BI SAM on copper.

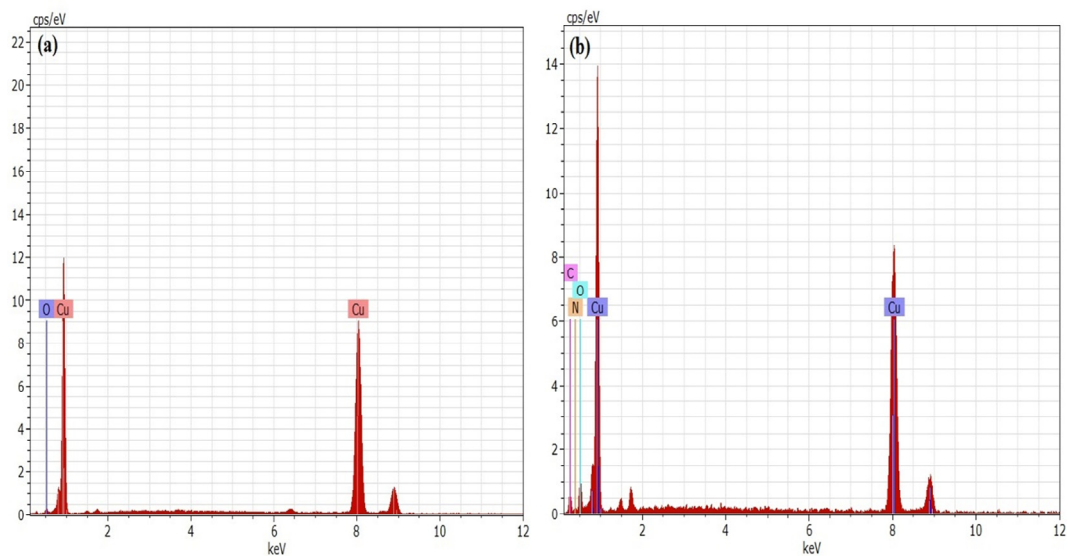


Fig. 2. EDX spectra of (a) polished and (b) BI SAM on copper

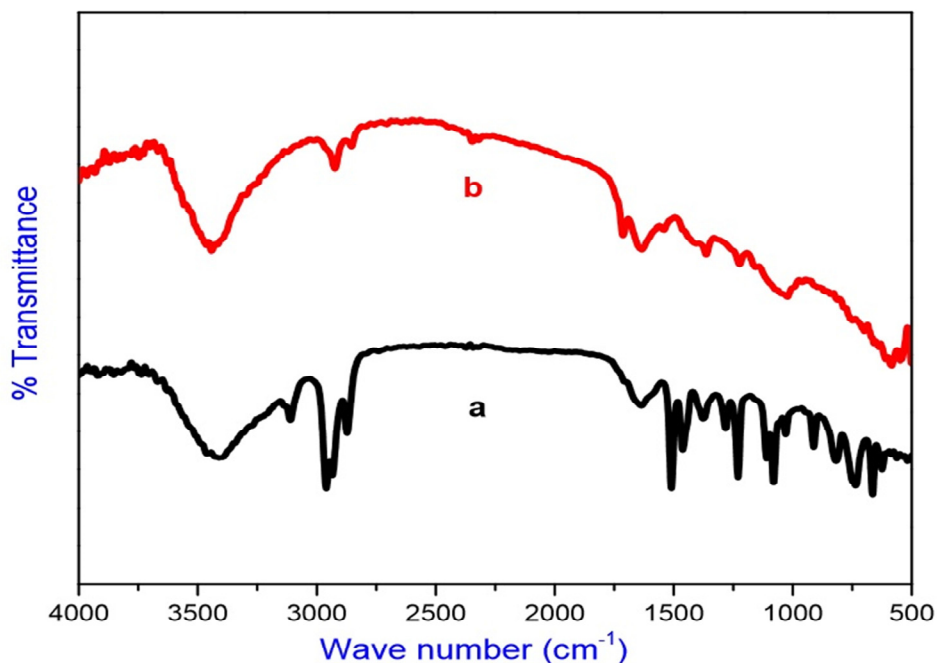


Fig. 3. FT-IR spectra of (a) pure BI and (b) BI SAM on copper

### 3.2. Evaluation of corrosion protection of copper by BI SAM

#### 3.2.1. Cyclic voltammometric studies

Fig. 4 shows the cyclic voltammograms obtained for bare copper and BI modified copper electrodes after immersion in 3% NaCl solution for 1 h, respectively. For the bare copper electrode (plot-a), there are two oxidation peaks at 0.19 V assigned as  $A_1$  and 0.35 V assigned as  $A_2$  in the forward scan, respectively. The one large reduction peak is observed at -0.36 V assigned as C in the reverse scan. The first oxidation peak ( $A_1$ ) is attributed to the formation of CuCl salt layer via oxidation of Cu(0) to Cu(I) as described by reaction (1) and the second oxidation peak ( $A_2$ ) is related to the oxidation of Cu(I) to soluble Cu(II) species, respectively (Eq. 2), [21]. In the reverse scan, the large reduction peak (C) corresponds to the reduction of CuCl to Cu.

The anodic copper dissolution mechanism in a chloride media has been widely investigated by a large number of scientists [22,23]. Copper metal is ionized via an electron transfer under the influence of  $\text{Cl}^-$  to form a CuCl layer at the copper surface.



where CuCl on copper surface has weak adhesion, partially protects the copper surface and on further attack by  $\text{Cl}^-$  is transformed into the soluble species ( $\text{CuCl}_2^-$ ).



When comparing the CV of the BI SAM modified copper (plot-b) with the bare copper, the oxidation and reduction peak currents are suppressed significantly. These results therefore indicate that the BI monolayer on the copper electrode affects the oxidation and reduction currents which demonstrate the inhibition of oxidation and reduction process of copper. Thus, CV studies provided the evidence for protection of copper against corrosion in 3% NaCl solution.

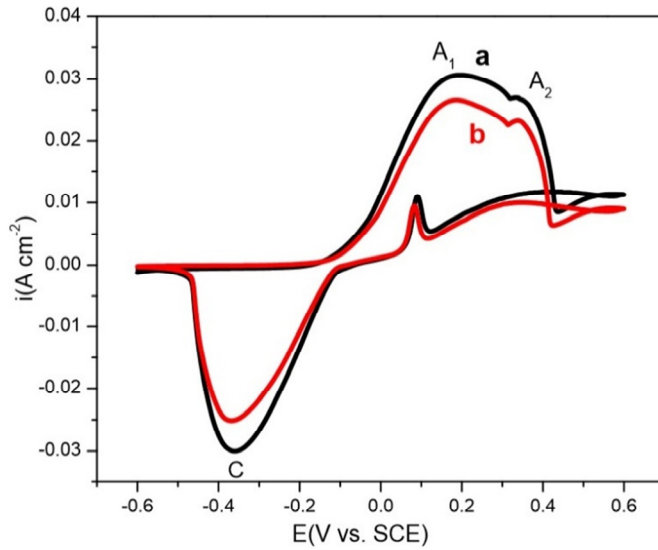


Fig. 4. Cyclic voltammograms curve for (a) bare and (b) BI SAM modified copper in 3% NaCl solution

3.2.2. Potentiodynamic polarization studies

Fig. 5 shows the potentiodynamic polarization curves of the bare copper and the BI coated copper electrodes in 3% NaCl solution. Various polarization parameters like corrosion potential ( $E_{corr}$ ), corrosion current density ( $i_{corr}$ ), anodic Tafel slope ( $b_a$ ) and cathodic Tafel slope ( $b_c$ ) obtained from Fig. 5 and their values are tabulated in Table 1. The percentage of inhibition efficiency was calculated using the following equation [24].

$$IE(\%) = \frac{i_{corr}^0 - i_{corr}}{i_{corr}^0} \times 100 \tag{3}$$

Where  $i_{corr}^0$  and  $i_{corr}$  are the corrosion current densities of the unmodified and modified BI SAM copper in 3% NaCl solution, respectively.

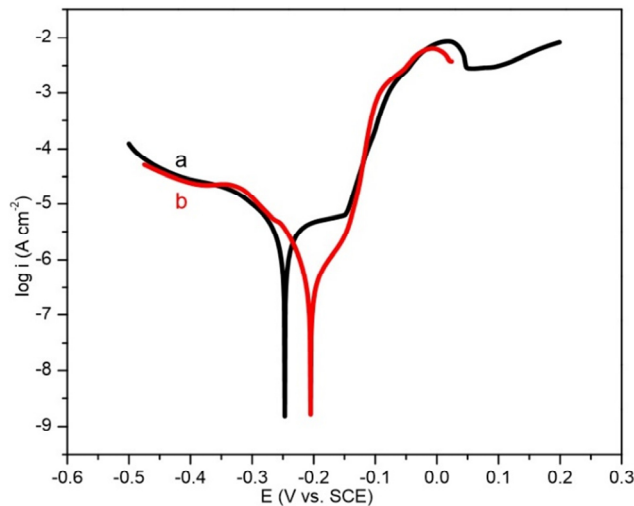


Fig. 5. Polarization curves obtained in 3% NaCl solution for (a) bare and (b) BI SAM modified copper

From the Tafel curves shown in Fig.5, it can be seen that for the copper with BI SAM, the anodic and cathodic currents are reduced significantly while corrosion potential ( $E_{\text{corr}}$ ) is shifted to more anodic (positive) region compared with that of the bare electrode.  $E_{\text{corr}}$  value for bare copper is  $-247$  (mV/SCE) while for the BI SAM modified copper is shifted to  $-205$  (mV/SCE). The results indicate that the BI behave as mixed type inhibitor predominantly inhibiting the anodic reaction than that of the cathodic reaction. The corrosion current ( $i_{\text{corr}}$ ) for bare copper is  $4.52 \mu\text{A cm}^{-2}$  which is significantly decreased to  $0.313 \mu\text{A cm}^{-2}$ , for BI SAM electrodes corresponding to the protection efficiency of 93.1%. The reduction of  $i_{\text{corr}}$  value and a positive shift in  $E_{\text{corr}}$  suggests that the formation of SAM has greatly improved the corrosion resisting property on the electrode surface resulting in hardly attack of aggressive ions to copper surface.

Table 1. Potentiodynamic polarization parameters obtained in 3% NaCl for the bare copper and copper electrode modified in 1.0 mM BI solution at assembly time for 24 h

C (mM)	$-E_{\text{corr}}$ (mV/SCE)	$I_{\text{corr}}$ ( $\mu\text{A cm}^{-2}$ )	$b_a$ (mV dec $^{-1}$ )	$b_c$ (mV dec $^{-1}$ )	IE (%)
0	247	4.524	90	201	-
1.0	205	0.313	21	95	93.1

### 3.2.3. Scanning Electron Microscopy (SEM) Studies

The SEM micrograph obtained for the bare copper and SAM coated copper after 3 days exposure in 3% NaCl solution is shown in Fig. 6 As can be seen clearly from Fig 6a, SEM micrographs show that the surface of bare in corrosive medium is highly damaged resulting in the surface layer extensively roughened due to permeation of water, aggressive chloride ion onto the copper surface. On the other hand, the appearance of SAM modified surface shows different morphological characterizes before and after immersion in 3% NaCl solution for 3 days. As compared with the bare surface, the BI SAM coated copper (Fig. 6b), surface seems to be relatively even and less damage on the copper surface. Observed findings clearly shows that the copper surface covered with a dense protective film which effectively protected the surface being corroded from the attack of aggressive environments.

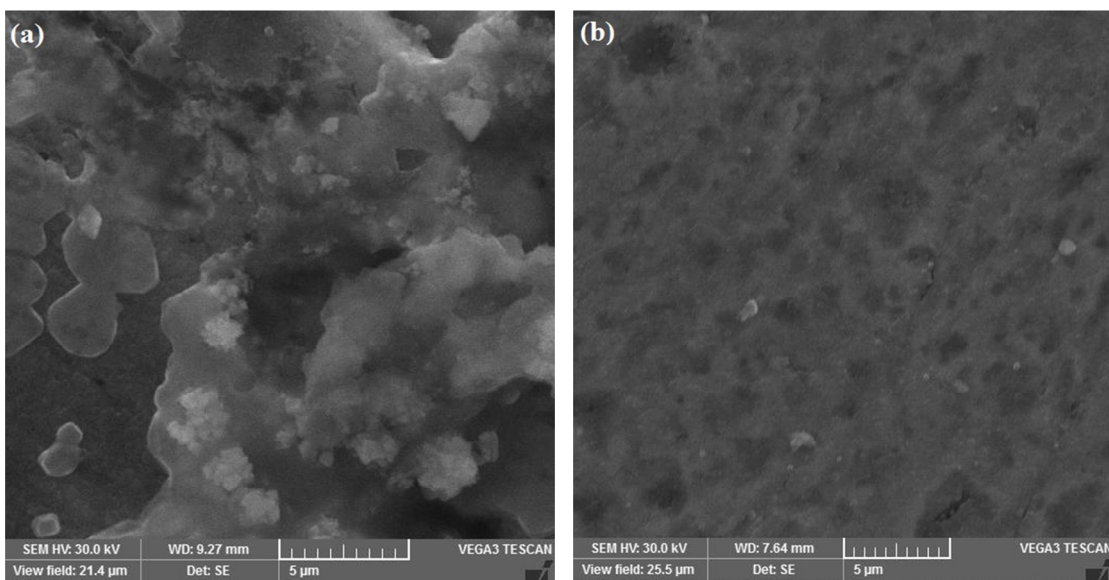


Fig. 6. SEM images of (a) bare and (b) BI SAM modified copper after immersed in 3% NaCl solution for 3 days

### 3.3. Evaluation of corrosion protection of copper by BI SAM

#### 3.3.1. Effect of BI concentration on the SAM formation

EIS as a technique is a nondestructive and informative method, has been widely used for the assessment of coatings for corrosion inhibition, particularly for analyzing the metal with SAMs. Fig. 7 shows the Nyquist impedance plots of bare copper and BI coated copper electrodes after 24 h of assembly in various concentrations of BI solution. As can be seen from the Nyquist plots shown in Fig. 7a inset, bare copper presents a conspicuous capacitive loop in the high frequency region followed by a straight line (Warburg impedance) at the low frequency zones. The high frequency capacitive loop is generally attributed to the time constant of charge transfer resistance ( $R_{ct}$ ) and double layer capacitance ( $C_{dl}$ ). The low frequency straight line portion which signifies the transport of soluble products species ( $CuCl_2^-$ ) from the electrode interface to the bulk solution or the transport of dissolved oxygen ( $O_2$ ) from the bulk solution to the surface of the copper substrate [9].

As seen from Fig.7 the size and shapes of the Nyquist impedance plots for the BI SAM coated copper electrode are significantly different from that of the bare electrode one. For the copper with SAM, the Warburg impedance is disappeared at low frequency in the Nyquist plots, implying the tightly packed layer to preclude the dissolution of copper and the diffusion of oxygen or chloride ions to the copper surface. As a result, the plots display several convex arcs from high to low frequency zone. In addition to that, the diameter of the curve more and more increased with enhancing the BI concentration, indicates that the thick barrier layer gradually tend to be forms on the electrode surface has got more resistance resulting better surface modification. Fig. 8 presents the Bode plots of the copper with and without SAM in 3% NaCl solution. Bode plots of SAM coated copper (Fig. 8a) shows the highest phase angle at high frequency region. It is also sensed that increasing the concentration of BI results in an increase in the maximal phase value, which indicates inhibition of the corrosion process. Bode plot (Fig. 8b) of SAM electrode display a high impedance modulus in low frequency relative to the bare one, which indicates that the superior corrosion protection performance.

The electrochemical equivalent circuit models used to fit the experimental results are shown in Fig. 10 (inset). The elements of the equivalent circuit includes consist of solution resistance ( $R_s$ ), charge transfer resistance ( $R_{ct}$ ), the resistance of the BI SAM ( $R_{sam}$ ) Warburg impedance (W), capacitance of the SAM ( $CPE_{sam}$ ) and capacitance of the double layer ( $CPE_{dl}$ ) are listed in Table 2. Considering the roughness and non-homogeneity of the substrate surface, a constant phase element (CPE) is modify for the capacitor to exactly fit the impedance data [25]. The impedance function of a CPE is described as follows.

$$Z_{CPE} = \frac{1}{Y_0 (j\omega)^{-n}} \quad (4)$$

where  $Y_0$  is the modulus,  $\omega$  the angular frequency,  $j$  is the imaginary root, and  $n$  is the exponential term which can be used as a measure of the inhomogeneity or roughness of the electrode surface.  $n$  is the phase shift and its value lies between 0 and 1. The smaller the value of  $n$ , the rougher the electrode surface and the more serious corrosion. The percentage of inhibition efficiency (IE %) is calculated using equation.

$$IE(\%) = \frac{R_{ct} - R_{ct}}{R_{ct}} \times 100 \quad (5)$$

where  $R_{ct}$  is the charge transfer resistance of the SAM coated copper and  $R_{ct}$  is the charge transfer resistance of the bare copper, respectively.

An examination from Table 2, it is clear that the value of the charge transfer resistance ( $R_{ct}$ ) of the bare is the lowest value. When the copper modified with BI SAM, the  $R_{ct}$  value increased remarkably as well as increase as the assembly concentration of BI. It indicates the higher packing of BI molecule on the electrode surface resulting in inhibit the electron transfer at the metal - solution interface. The decreases in capacitance values in presence of SAM due to covering of BI molecules on the active sites at the electrode surface resulting fall in local dielectric constant and/or an increase in the thickness of the double layer. The change of  $n$  value may be ascribed to the increase of BI concentration resulted in a variation of electrode surface roughness. It is seen that the  $R_{ct}$  value increased from 6.981  $k\Omega\text{ cm}^2$  to 9.445  $k\Omega\text{ cm}^2$  in the BI solution from 0.1 to 1.0 mM. Therefore, the SAM formed in this concentration

more compact. It also observed that percentage of inhibition efficiency increased with increasing concentration of the BI. Apparently, higher concentration of SAM solution leads to more compact formation monolayer on the electrode surfaces. The high  $R_{ct}$  and lower CPE value obtained at 1.0 mM of BI, therefore chosen as the optimum concentration to form barrier film on copper surface.

Table 2. Nyquist impedance parameters obtained in 3% NaCl for the bare and copper electrodes modified in various concentrations of BI solution at assembly time for 24 h

C (mM)	$R_{ct}$ ( $k\Omega\text{ cm}^2$ )	$CPE_{dl}$ ( $\mu\text{F cm}^{-2}$ )	$n_1$	$R_{sam}$ ( $k\Omega\text{ cm}^2$ )	$CPE_{sam}$ ( $\mu\text{F cm}^{-2}$ )	$n_2$	IE (%)
0	0.806	97.06	0.68	-	-	-	-
0.1	6.981	80.22	0.42	1.952	23.64	0.84	88.5
0.5	8.724	59.83	0.40	2.286	19.37	0.85	90.8
1.0	9.445	53.91	0.44	3.356	14.43	0.87	91.5

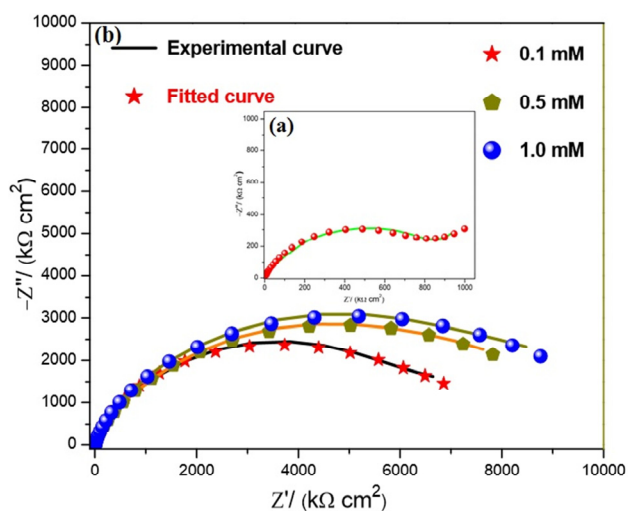


Fig. 7. Impedance spectra recorded in 3% NaCl for (a) bare and (b) copper electrode modified in different concentrations of BI solution for 24 h.

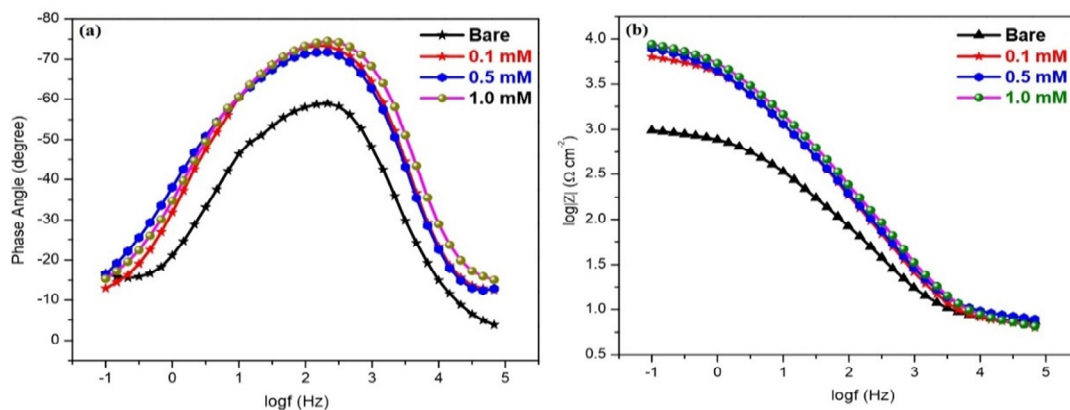


Fig. 8. Bode plots of (a) bare and (b) BI SAM modified copper after 24 h of assembly in different concentrations of BI solution.

### 3.3.2. Effect of assembly time

Fig. 9 shows the Nyquist impedance spectra of the BI modified copper in 3% NaCl solution. The impedance parameters obtained from the electrochemical equivalent circuit plots are tabulated in Table 3. When the copper modified with (1.0 mM) BI for 1 h, the observed  $R_{ct}$  value is 2.879  $k\Omega\text{ cm}^2$  with the efficiency was 72.0%. This result suggests that the formation of BI SAM on surface is poorly packing density. With an increase in assembly time from 6 to 12 h, the  $R_{ct}$  value increased from 5.335 to 7.693  $k\Omega\text{ cm}^2$ . Further, on assembly time was raised to 12 to 24 h, there is a large increase in the  $R_{ct}$  value which is 9.445  $k\Omega\text{ cm}^2$  and the inhibition efficiency is 93.2% and further prolonging assembly time step up to 30 h, there is a no considerable increase in the  $R_{ct}$  value which is 9.926  $k\Omega\text{ cm}^2$ . By increasing assembling time, more number of BI molecule adsorbed on electrode surface and forming of SAM with fewer defects. Therefore, the assembly process, involves the initial BI molecules in the solution adsorb on the substrate surface rapidly and after that, the adsorbed molecules will rearrange form a thicker film gradually. The  $R_{ct}$  values at the assembly time of 24 and 30 h are similar and it shows that the formations of BI monolayer on copper have attained a dense and more orderly state after the assembling for 24 h. Further, increase in assembly time does not show any significant effect on inhibition efficiency of the SAM. It is also found that the CPE values are decreased from 62.28 to 8.58 and the  $n$  value is increased from 0.46 to 0.52. Therefore, best assembly time chosen as 24 h for SAM formation on copper surface.

Table 3. Nyquist impedance parameters obtained in 3% NaCl for the bare and copper electrode modified in 1.0 mM BI solution at different assembly time

t (h)	$R_{ct}$ ( $k\Omega\text{ cm}^2$ )	$CPE_{dl}$ ( $\mu\text{F cm}^{-2}$ )	$n_1$	$R_{sam}$ ( $k\Omega\text{ cm}^2$ )	$CPE_{sam}$ ( $\mu\text{F cm}^{-2}$ )	$n_2$	IE (%)
0	0.806	97.06	0.68	-	-	-	-
2	2.879	62.28	0.46	5.85	17.26	0.83	72.0
6	5.335	48.23	0.48	1.931	13.81	0.86	84.9
12	7.693	45.37	0.49	2.256	15.03	0.88	89.5
24	9.445	53.91	0.44	3.356	14.43	0.87	91.5
30	9.926	8.58	0.52	5.497	26.27	0.89	91.9

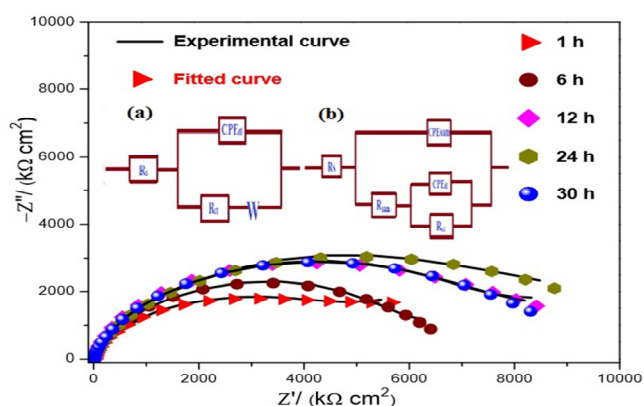


Fig. 9. Impedance spectra obtained in 3% NaCl for (a) bare and (b) BI SAM modified copper electrodes at different assembly time (Inset Fig. (a), (b) for the circuit of bare and BI SAM modified copper).

#### 4. Conclusion

In this paper, we reported the formation BI SAM on copper surface for corrosion inhibition. EIS has been used to establish the optimum concentration and assembly time of the BI SAM and it was found that the BI SAM was formed at 24 h assembly time with 1.0 mM BI. The BI SAM formed on copper is characterized by FT-IR and EDX which are clearly infers the chemisorption of BI molecule on copper surface through nitrogen atoms. Potentiodynamic polarization curve indicate that the BI acts as a mixed inhibitor that mainly inhibit the anodic reaction. The surface morphology of BI modified copper immersed in 3% NaCl was smoother than that of the bare copper, indicating successful corrosion inhibition.

#### Acknowledgements

P. Durainatarajan is grateful to the UGC-RFSMS (Research Fellowship in Sciences for Meritorious Students, grant No: F.No.25-1/2014-15/(BSR)/7-225/2008/(BSR), dt: 7th October 2015) for financial support and also the authorities of Gandhigram Rural Institute for encouragement.

#### References

- [1] A. Ulman, Chem. Rev. 96 (1996)1533–1554.
- [2] C.T. Wang, S.H. Chen, H.Y. Ma, C.S. Qi, J. Appl. Electrochem. 33 (2003) 179–186.
- [3] W. Chen, S. Hong, H.B. Li, H.Q. Luo, M. Li, N.B. Li, Corros. Sci. 61 (2012) 53–62.
- [4] G.K. Jennings, J.C. Munro, T.H Yong, P.E. Laibinis, Langmuir 14 (1998) 6130–6139.
- [5] L. Núñez, E. Reguera, F. Corvo, E. Gonzalez, C. Vazquez, Corros. Sci. 47 (2005) 461–484.
- [6] A. El Warraky, H.A. El Shayeb, E.M. Sherif, Anti-Corros. Meth. Mater. 51 (2004) 52–61.
- [7] P.E. Laibinis, G.M. Whitesides, J. Am. Chem. Soc. 114 (1992) 9022–9028.
- [8] Y.Q. Feng, W.K. Teo, K.S. Siow, Z.Q. Gao, K.L. Tan, A.K. Hsieh, J. Electrochem. Soc. 144 (1997) 55–64.
- [9] A.T. Lusk, G.K. Jennings, Langmuir 17 (2001) 7830–7836.
- [10] F. Caprioli, M. Beccari, A. Martinelli, V.D. Castro, F. Decker, Phys. Chem. Chem. Phys. 12 (2010) 9230–9238.
- [11] Z.L. Quan, S.H. Chen, Y. Li, X.G. Cui, Corros. Sci. 44 (2002) 703–715.
- [12] Y. Zhou, S. Xu, L. Guo, S. Zhang, H. Lu, Y. Gong, F. Gao, RSC Adv., 5 (2015) 14804–14813.
- [13] D.Q. Zhang, X.M. He, Q.R. Cai, L.X. Gao, G.S. Kim, J. Appl. Electrochem. 39 (2009) 1193–1198.
- [14] C. Hao, R.H. Yin, Z.Y. Wan, Q.J. Xu, G.D. Zhou, Corros. Sci. 50 (2008) 3527–3533.
- [15] F. Sinapi, J. Delhalle, Z. Mekhalif, Mater. Sci. Eng., C 22 (2002) 345–353.
- [16] Y. Qiang, S. Zhang, S. Xu, L. Yin, RSC Adv., 5 (2015) 63866–63873.
- [17] L. Feng, H. Yang, F. Wang, Electrochimica. Acta 58 (2011) 427–436.
- [18] B.V. Appa Rao, M. Narsihma Reddy, Arab. J. Chem. (2014) <http://dx.doi.org/10.1016/j.arabjc.2013.12.026>.
- [19] A. Dafali, B. Hammouti, A. Aouniti, R. Mokhlisse, S. Kertit, K. Elkacemi, Ann. Chim. Sci. Mat. 25 (2000) 437–446.
- [20] H. Otma i , E. Stupnišek-Lisac, Electrochim. Acta 48 (2003) 985–991.
- [21] D.G. Li, S.H. Chen, S.Y. Zhao, H.Y. Ma, Colloids Surf. A 273 (2006) 16–23.
- [22] C. Deslouis, B. Tribollet, G. Mengoli, M.M. Musiani, J. Appl. Electrochem. 18 (1988) 374–383.
- [23] G. Kear, B.D. Barker, F.C. Walsh, Corros. Sci. 46 (2004) 109–135.
- [24] P. Wang, C. Liang, B. Wu, N. Huang, J. Li, Electrochim. Acta 55 (2010) 878–883.
- [25] X. Wu, H. Ma, S. Chen, Z. Xu, A. Sui, J. Electrochem. Soc. 146 (1999) 1847–1853.